

Temperature and final state effects in radio frequency spectroscopy experiments on atomic Fermi gases

Yan He, Chih-Chun Chien, Qijin Chen, and K. Levin

James Franck Institute and Department of Physics, University of Chicago, Chicago, Illinois 60637

(Dated: May 27, 2019)

We present a formalism for addressing radio frequency (RF) spectroscopy experiments in homogeneous atomic Fermi gases in the presence of pairing, but not necessarily superfluidity, and at finite temperatures, T . Our approach includes final state effects and our calculated spectra satisfy the zeroth- and first-moment sum rules at all T . We show how the continuum and bound state contributions depend significantly on T , and explain recent RF experiments on “bound-bound” transitions. We make predictions for future experiments.

PACS numbers: 03.75.Hh, 03.75.Ss, 74.20.-z

arXiv:0804.1429

The superfluid and normal phases in trapped Fermi gases are presenting us with novel states of matter in which there appears to be pairing independent of superfluid order. This feature is suggestive of similar behavior in the high temperature cuprates [1]. The pairing gap (in ${}^6\text{Li}$) is best probed using radio frequency (RF) spectroscopy [2, 3] which focuses on the three lowest energy atomic hyperfine states (two of which are involved in the pairing, while a third provides a final excited state for one component of a broken pair). RF techniques have now been widely applied experimentally [2, 3, 4]. Theoretical work has been most extensive for cases in which the interaction between the final excited state and the superfluid is neglected [5, 6, 7, 8]. Recent inclusion of these final state effects [9, 10, 11, 12, 13] is now of considerable interest but has been focused on low or zero temperature.

In this paper, we argue that, just as in the standard BCS theory of superconductivity, temperature effects are an essential component of any theoretical framework. Thus theoretical predictions will provide the basis for future tests of alternative approaches to the crossover. A central contribution of the present work is to show how to include $T \neq 0$ in the theory of RF experiments in homogeneous gases, and to address recent experiments as well as predict features for future measurements. Thereby, we help lay the foundation for systematically measuring the pairing gap from above to below T_c .

In this regard, one can think of these experimental studies as the counterpart of the important temperature dependent photoemission experiments in high temperature superconductors [1]. Indeed, a striking feature of these Fermi gases at unitarity was observed very early on [14]: it is difficult to establish where (and if) the superfluid transition T_c occurs. This behavior is in contrast to the BCS and BEC cases. For the former a pairing gap sets in abruptly at T_c and for the latter, there are clear superfluid signatures associated with bimodality within the density profiles. One can see how the presence of a normal state pairing gap at unitarity, which leads to an apparent gradual onset of superfluidity, will obscure signatures of T_c .

The theoretical approach adopted here is based on a finite temperature theory of BCS-BEC crossover [1, 15] which reduces to the BCS-Leggett equations at $T = 0$. This approach is the simplest in a hierarchy of schemes [16, 17, 18] which include bosonic fluctuations (or noncondensed pairs) and has several advantages. Among others, this ground state has been

successfully applied to address “final state effects” in RF spectroscopy [12]. Importantly, for addressing T_c signatures, there are no first order transitions at T_c which are found in alternative theories, for example, in those based on the Nozières-Schmitt-Rink scheme [19].

We consider a superfluid of pairs in the equally populated hyperfine 1-2 levels and apply a radio frequency ω_{23} to excite the atoms in state 2 to state 3. We formulate the finite T , RF problem using a diagrammatic scheme which can be made compatible with the diagrams in Ref. 11, although attention in that paper was restricted to very low temperatures. We will show below that our diagrammatic scheme reduces at $T = 0$ to the scheme of Ref. 12. This correspondence, and indeed, all diagrammatic formulations [10] of the RF experiments are based on a T -matrix approach. The T -matrix used here (for the 1-2 channel) is consistent with the BCS-Leggett ground state equations. This requires, as we have discussed before [1], a T -matrix which consists of one bare and one dressed Green’s function. We have

$$t_{12}^{-1}(Q) = g_{12}^{-1} + \sum_K G_1(K)G_2^0(Q - K) \quad (1)$$

$$t_{13}^{-1}(Q) = g_{13}^{-1} + \sum_K G_1(K)G_3^0(Q - K) \quad (2)$$

where we have introduced the dressed Green’s function $G = [(G^0)^{-1} - \Sigma]^{-1}$ and G^0 is the Green’s function of the non-interacting system. Here the subscripts indicate the hyperfine levels, $K \equiv (i\omega_l, \mathbf{k})$, $Q \equiv (i\Omega_n, \mathbf{q})$ are 4-momenta with $\sum_K \equiv T \sum_l \sum_{\mathbf{k}}$, etc., and ω_l and Ω_n are fermion and boson Matsubara frequencies, respectively. Throughout we take $\hbar = k_B = 1$ and assume a contact potential (so that the strict Hartree self-energy vanishes) and a (nearly) empty population in the hyperfine 3 state so that $G_3(K) \approx G_3^0(K)$. As has been demonstrated elsewhere [1], it is reasonable to take the self energy (on the real frequency axis) in the Green’s functions G_1 and G_2 to be of the generalized BCS form

$$\Sigma(\omega, \mathbf{k}) \approx \frac{\Delta^2}{\omega + \epsilon_{\mathbf{k}}} \quad (3)$$

Similarly, we have shown [20] that, below T_c , $\Delta(T)$ is constrained by a BCS-like gap equation which can be written as $1 + g_{12}\chi_{12}(0) = 0$ where $\chi_{12}(Q) = \sum_K G_1(K)G_2^0(Q - K)$,

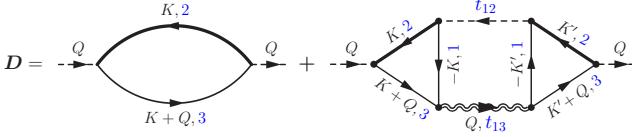


Figure 1: (Color online) Feynman diagrams for the RF response function $D(Q)$. The left bubble is the lowest order D_0 , whereas the right diagram, D_{AL} , is associated with final state effects. Here thin (thick) lines stand for bare (full) fermion propagators, the dashed line for t_{12} , approximated as the condensate, and double wiggly line for t_{13} . The numbers in blue indicate the hyperfine levels.

in conjunction with a fermion number equation. More generally, the propagator for noncondensed pairs is of the form $t_{12}(Q) = g_{12}/[1 + g_{12}\chi_{12}(Q)]$.

In our diagrams we avoid the direct use of Gor'kov F functions because at finite T there is ambiguity associated with the distinction between the pairing gap (which we call Δ) and the order parameter, called Δ_{sc} . The difference between these two energy scales can be shown [1] to be associated with non-condensed pair effects which enter as

$$\Delta_{pg}^2(T) = \Delta^2(T) - \Delta_{sc}^2(T). \quad (4)$$

Here we note that $\Delta_{pg}^2 = -\sum_{Q \neq 0} t_{12}(Q)$ which allows T_c to be determined [1] as the temperature where Δ_{sc} first vanishes. It is, nevertheless convenient notationally to define a form of Gor'kov F function in terms of the pairing gap as

$$\Delta G_2(K) G_1^0(-K) = \frac{\Delta}{\omega_l^2 + E_k^2} \equiv F(K),$$

where $E_k = \sqrt{\xi_k^2 + \Delta^2(T)}$, and $\xi_k = \epsilon_k - \mu$, $\epsilon_k = k^2/2m$. Because of the constraints imposed by the gap equation, $t_{12}(Q)$ diverges at $Q = 0$ so that it is reasonable to set Q in t_{12} to zero, i.e., $t_{12}(Q) \approx -(\Delta^2/T)\delta(Q)$. This assumption, which leads to the simple form of Eq. (3), is not essential for understanding the physics but it does greatly simplify the calculations [21].

The resulting diagram set is shown in Fig. 1 and this last approximation is equivalent to treating the Aslamazov-Larkin (AL) diagram (called D_{AL}) in Fig. 1 at the BCS mean-field level, leading to the opposite momenta $\pm K$ for particles 1 and 2 in the diagram. The leading order term, $D_0(Q)$, of the response function (called $D(Q)$) appears as the bubble on the left and was introduced in Ref. 5. The term on the right, $D_{AL}(Q)$, depends on Δ , not Δ_{sc} , and incorporates final-state effects via the interactions g_{12} between 1 and 2 and g_{13} between 1 and 3. We neglect the effects arising from the interaction between 2 and 3. This is consistent with the approach in Ref. 9. This second term has appeared previously in studies of the superfluid density [15].

Writing out the AL diagram yields

$$D_{AL}(Q) = \left[\sum_K F(K) G_3^0(K+Q) \right]^2 t_{13}(Q). \quad (5)$$

For the RF field, $Q = (i\Omega_n, \mathbf{0})$ so that $D(i\Omega_n) \equiv D(Q)$. We take μ_3 satisfying $f(\xi_{k,3}) = 0$, where $\xi_{k,3} = \epsilon_k - \mu_3$.

Then the RF current, given by the retarded response function, is $I(\nu) \equiv -(1/\pi) \text{Im} D^R(\Omega)$, where $\Omega \equiv \nu + \mu - \mu_3$, and we find

$$D(Q) = D_0(Q) + \frac{[D_2(Q)]^2}{m/4\pi a_{13} + D_1(Q)}, \quad (6)$$

and $t_{13}^{-1}(Q) = m/4\pi a_{13} + D_1(Q)$, where a_{13} (and a_{12}) are the s -wave scattering length in the 1-3 (and 1-2) channels, respectively. Here $D_0(Q) = \sum_K G_2(K) G_3^0(K+Q)$

$$= \sum_K \left[\frac{f(E_k) - f(\xi_{k,3})}{i\Omega_n + E_k - \xi_{k,3}} u_k^2 + \frac{1 - f(\xi_{k,3}) - f(E_k)}{i\Omega_n - E_k - \xi_{k,3}} v_k^2 \right] \quad (7)$$

and $I_0(\nu) = -(1/\pi) \text{Im} D_0^R(\Omega)$. We also define $D_2(Q) \equiv \sum_K F(K) G_3^0(K+Q)$

$$= \sum_K \frac{\Delta}{2E_k} \left[\frac{1 - f(E_k) - f(\xi_{k,3})}{i\Omega_n - E_k - \xi_{k,3}} - \frac{f(E_k) - f(\xi_{k,3})}{i\Omega_n + E_k - \xi_{k,3}} \right] \quad (8)$$

and $D_1(Q) \equiv \sum_K G_1(K) G_3^0(Q-K) - \sum_{\mathbf{k}} (1/2\epsilon_k) =$

$$\sum_K \left[\frac{f(E_k) + f(\xi_{k,3}) - 1}{i\Omega_n - E_k - \xi_{k,3}} u_k^2 + \frac{f(\xi_{k,3}) - f(E_k)}{i\Omega_n + E_k - \xi_{k,3}} v_k^2 \right] - \sum_{\mathbf{k}} \frac{m}{k^2}. \quad (9)$$

After analytical continuation and change of variable, we have $\Omega \pm E_{\mathbf{k}} - \xi_{k,3} = \nu \pm E_{\mathbf{k}} - \xi_k$. It is clear that the denominators here are the same as those which appear in t_{12} . Furthermore, at $\nu = 0$, $f(\xi_{k,3})$ is cancelled out so that

$$t_{13}^{-1}(0) = (g_{13}^{-1} - g_{12}^{-1}) + t_{12}^{-1}(0) = g_{13}^{-1} - g_{12}^{-1}. \quad (10)$$

It follows that the complex functions $D_0(Q)$, $D_1(Q)$, and $D_2(Q)$ are the same as their wave function calculation counterparts [12] when the pairing gap Δ is chosen to be order parameter Δ_{sc} and $T = 0$. It is ν not Ω that should be identified with the experimental RF detuning.

After some straightforward algebra, one can show that when $g_{13} = g_{12}$ there is an exact cancellation such that $I(\nu) \sim \delta(\nu)$. In general, we have $I_0(\nu) = (1/\pi)(\Delta^2/\nu^2) \text{Im} \bar{t}_{13}^{-1,R}(\nu)$, and

$$\begin{aligned} I(\nu) &= \left[\frac{1}{g_{12}} - \frac{1}{g_{13}} \right]^2 \frac{I_0(\nu)}{|\bar{t}_{13}^{-1,R}(\nu)|^2} \\ &= -\frac{1}{\pi} \left[\frac{m}{4\pi a_{13}} - \frac{m}{4\pi a_{12}} \right]^2 \frac{\Delta^2}{\nu^2} \text{Im} \bar{t}_{13}^R(\nu), \end{aligned} \quad (11)$$

where $\bar{t}_{13}^R(\nu) \equiv t_{13}^R(\Omega)$.

Equation (5) makes it clear that final state effects in the RF current directly reflect the T -matrix in the 1-3 channel. If there are bound states associated with poles in $t_{13}^R(\Omega)$, these will show up as sharp structure in the current associated with the so-called ‘‘bound-bound’’ transition. Similarly, structure in the T -matrix t_{12} of the paired states is reflected in the self energy contribution of the Green's function G_2 which appears in the leading order contribution to the RF current. This latter effect has been shown to be important [10, 22] in the context

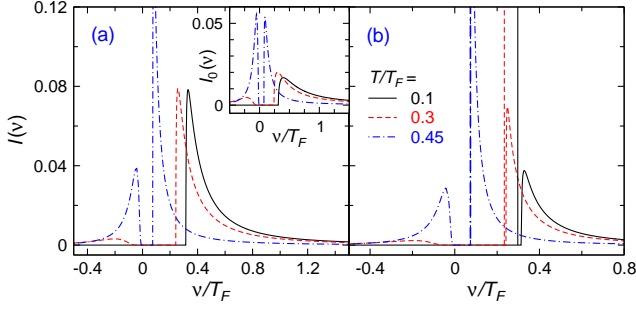


Figure 2: (Color online) RF current $I(\nu)$ as a function of RF detuning ν for transitions from unitarity $1/k_F a_{12} = 0$ to final state (a) $1/k_F a_{13} = -1$ and (b) -0.5 in the BCS regime, at $T/T_F = 0.1$ (Black solid), 0.3 (red dashed) and 0.45 (blue dot-dashed lines). The sharp lines next to the right continuum in (b) correspond to bound states. Inset: Lowest order RF current $I_0(\nu)$ vs ν .

of gases which are so strongly polarized that superfluidity is driven away [4]. In this case the T -matrix in Eq. (4) is based on $\chi_{12}^0(Q) = \sum_K G_1^0(K)G_2^0(Q-K)$ which contains two bare Green's functions and, therefore, effects not considered here. Studies of this function in the polarized case show a pole [10, 22] in t_{12} , which leads to a quasi-pairing-gap structure in the RF current, as observed [4]. These remarks illustrate that a number of results from the literature can be consolidated into a generalized T -matrix formalism.

Of importance, in assessing a theoretical framework for computing the RF current are the two sum rules associated with the total integrated current and the first moment or ‘‘clock shift’’ [9]. Using the Kramers-Kronig relations between $\text{Re } t_{13}^R$ and $\text{Im } t_{13}^R$, it is easy to prove that, not only in the ground state, but also at finite temperature, Eq. (11) satisfies

$$\int d\nu I(\nu) = n_2 - n_3, \quad (12)$$

$$\int d\nu \nu I(\nu) = \Delta^2 \frac{m}{4\pi} \left(\frac{1}{a_{12}} - \frac{1}{a_{13}} \right), \quad (13)$$

where n_2 and $n_3 (= 0)$ are the density of state 2 and 3 atoms, respectively. In this way we find for the clock shift

$$\bar{\nu} = \frac{\int d\nu \nu I(\nu)}{\int d\nu I(\nu)} = \frac{\Delta^2}{n_2 - n_3} \frac{m}{4\pi} \left(\frac{1}{a_{12}} - \frac{1}{a_{13}} \right). \quad (14)$$

It should be stressed that this sum rule is satisfied only when $a_{13} \neq 0$ and both diagrammatic contributions are included. It is easy to show that at large ν , $I_0(\nu) \sim \nu^{-3/2}$, $\text{Im } t_{13}^R \sim \nu^{-1/2}$, so that $I(\nu) \sim \nu^{-5/2}$, in agreement with Ref. 11. Clearly, the first moment of $I(\nu)$ is integrable, whereas the first moment of $I_0(\nu)$ is not. Finally, Eq. (11) reveals that the spectral weight (including possible bound states) away from $\nu = 0$ will disappear when the gap Δ vanishes.

Now we can anticipate some of the key physical features associated with the poles and imaginary parts of Eqs. (6)-(9). In general, the RF spectrum may contain a bound state associated with poles at ν_0 in t_{13} , as determined by $t_{13}^{-1}(\nu_0) = 0$, along with a continuum spanned by the limits of $\nu = \xi_k \pm E_k$,

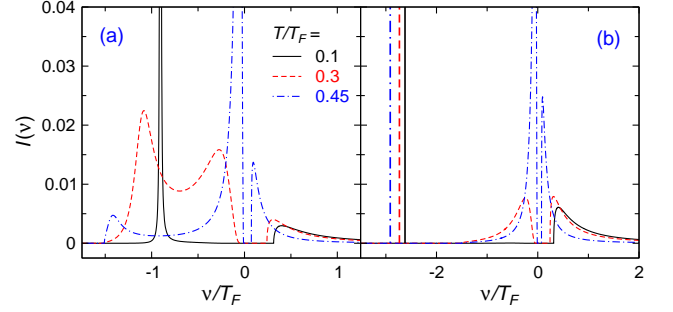


Figure 3: (Color online) RF current $I(\nu)$ as a function of detuning ν for transitions from unitarity $1/k_F a_{12} = 0$ to final states (a) $1/k_F a_{13} = 0.5$ and (b) $1/k_F a_{13} = 1$ in the BEC regime, at $T/T_F = 0.1$ (black solid), 0.3 (red dashed), and 0.45 (blue dot-dashed lines). The sharp vertical lines in (b) indicate bound states.

i.e., $-(\sqrt{\mu^2 + \Delta^2} + \mu) \leq \nu \leq 0$ and $\nu \geq \sqrt{\mu^2 + \Delta^2} - \mu$. The continuum at positive frequencies is primarily associated with breaking a pair in the condensate and promoting the state 2 to state 3. On the negative frequency side, the continuum is primarily associated with promoting to state 3 an already existing thermally excited 2 particle. Indeed, the spectral weight of the negative continuum vanishes at low T as $e^{-\Delta/T}$. Therefore, there is a strong asymmetry in the continuum with the bulk of the weight on the positive frequency side for low T . If the bound state falls within the negative continuum, it will acquire a finite life time, and decay quickly at high T .

Figures 2(a) and 2(b) show the behavior of the spectrum $I(\nu)$ when the initial state 1-2 pairing is at unitarity and the final state 1-3 pairing is on the BCS side of the 1-3 resonance, for temperatures $T/T_F = 0.1, 0.3,$ and 0.45 . The inset of Fig. 2(a) indicates the behavior in the absence of final state effects for the same temperatures. The asymmetry of the continuum around $\nu = 0$, discussed earlier, is evident even in the leading order bubble diagram. In Fig. 2(a), the final state interaction $1/k_F a_{13} = -1$ is relatively weak, and there is no bound state. In contrast, at $1/k_F a_{13} = -0.5$, a bound state emerges at low T as shown in Fig. 2(b), consistent with Basu and Mueller [12]. However, it disappears at moderate temperatures when the gap becomes small.

Figure 3 presents the analogous plots for RF transitions from an initial 1-2 pairing at unitarity to final 1-3 pairing on the BEC side of the 1-3 resonance with (a) $1/k_F a_{13} = 0.5$ and (b) $1/k_F a_{13} = 1$. Here in both cases there are bound states reminiscent of the ‘‘bound-bound’’ transition in the two-body system [23]. The binding energy for the latter case is fairly insensitive to temperature. Notably, however, for relatively weaker interactions $1/k_F a_{13} = 0.5$ in Fig. 3(a), the bound states fall within the negative continuum, and the behavior is quite distinctive. As T increases, the bound state decays rapidly. On the other hand, a peak at lower energy ($|\nu|$) right below $\nu = 0$ emerges, which is strongly enhanced by the factor $1/\nu^2$ in Eq. (11). The disappearance of the bound state with temperature is marked by a very unusual two-peaked spectrum in the negative frequency regime, which is seen at the two higher T . It will be of interest to search

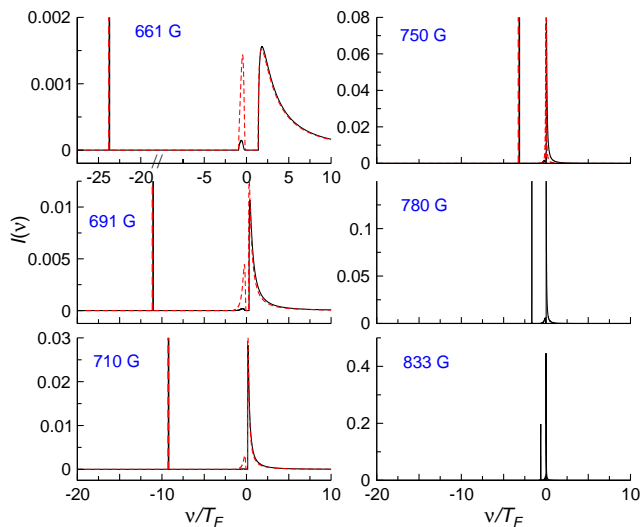


Figure 4: (Color online) RF current $I(\nu)$ as a function of detuning ν for a 1-3 superfluid with RF excitation from state 3 to state 2. The black curves are calculated at experimental parameters of $(1/k_F a_{13}, 1/k_F a_{12}, T/T_F) = (0.705, 3.493, 0.2)$, $(-0.01, 2.254, 0.14)$, $(-0.336, 2.00, 0.09)$, $(-0.707, 0.987, 0.09)$, $(-0.898, 0.522, 0.09)$, and $(-1.238, 0.011, 0.06)$ from low to high fields. The red dashed curves are calculated at twice the temperatures. The sharp lines on the left indicate bound states.

for such unusual behavior directly. The most plausible case is to use the 2-3 superfluid at resonance at 811.2 G [23] and drive state 3 to 1. At $E_F = 5 \sim 10$ kHz, which is about 2-4 times smaller than the typical values cited in [4], we have $1/k_F a_{12} = 0.32 \sim 0.45$, and expect to observe the double-peaked structure in $I(\nu)$ at $\nu < 0$. Both Figs. 2 and 3 show that the continuum spectral weight in $I(\nu)$ at $\nu < 0$ rises sub-

stantially with temperature, and may possibly dominate.

Finally, we turn in Fig. 4 to a slightly different paired state, which has also been studied experimentally [3]: the initial 1-3 superfluid with RF excitation from state 3 to state 2. Final state effects are then associated with a_{12} . The calculations for the black curves of $I(\nu)$ in all six panels were performed with experimental parameters, and should be compared with Fig. 4 of Ref. [3]. The red curves were obtained at twice the experimental temperatures. At the lowest field, 661 G, both $a_{13} > 0$ and $a_{12} > 0$. At 691 G, $1/a_{13} = 0$ (on resonance), but still $a_{12} > 0$. For higher fields, we have $1/a_{13} < 0 < 1/a_{12}$. At 833 G, 1-2 is essentially on resonance. As the field increases, the bound state binding energy decreases, and merges into the negative continuum at 780 G and 833 G. Note that $T_F \approx 20$ kHz, and that the sharp bound states will have instrumental spectral broadening, our calculated black curves can be seen to be in very good agreement with experiment. As a prediction, at higher T (red dashed lines), the negative ν continuum states start to become apparent.

In conclusion, we have shown that RF spectroscopy contains a rich array of information beyond a measurement of the pairing gap. Bound state effects are associated with final state interactions. The positive frequency continuum reflects the breaking up of pairs, thus revealing their dispersion. Of interest is the negative frequency continuum which is present at finite T and reveals the dispersion and characteristics of thermally broken pairs. BCS superconductivity has established a precedent for a comparison between theory and experiment at general T ; consequently the Fermi gases may provide a richer subject for study than the Bose gases, where theoretically, there are limitations [24] on addressing all T from unphysical first order transitions at T_c and other restrictions.

This work is supported by Grants NSF PHY-0555325 and NSF-MRSEC DMR-0213745. We thank S. Basu, C. Chin, and E. Mueller for helpful discussions.

-
- [1] Q. J. Chen, J. Stajic, S. N. Tan, and K. Levin, *Phys. Rep.* **412**, 1 (2005); K. Levin and Q. J. Chen, e-print cond-mat/0610006.
- [2] C. Chin, M. Bartenstein, A. Altmeyer, S. Riedl, S. Jochim, J. H. Denschlag, and R. Grimm, *Science* **305**, 1128 (2004).
- [3] C. Schunck, Y.-I. Shin, A. Schirotzek, and W. Ketterle, arXiv:0802.0341.
- [4] C. H. Schunck, Y. Shin, A. Schirotzek, M. W. Zwierlein, and W. Ketterle, *Science* **316**, 867 (2007).
- [5] J. Kinnunen, M. Rodriguez, and P. Törmä, *Science* **305**, 1131 (2004).
- [6] Y. He, Q. J. Chen, and K. Levin, *Phys. Rev. A* **72**, 011602(R) (2005).
- [7] P. Massignan, G. M. Bruun, and H. T. C. Stoof, *Phys. Rev. A* **77**, 031601(R) (2008).
- [8] Y. He, C.-C. Chien, Q. J. Chen, and K. Levin, *Phys. Rev. A* **77**, 011602(R) (2008).
- [9] Z. Yu and G. Baym, *Phys. Rev. A* **73**, 063601 (2006).
- [10] M. Punk and W. Zwerger, *Phys. Rev. Lett.* **99**, 170404 (2007).
- [11] A. Perali, P. Pieri, and G. C. Strinati, *Phys. Rev. Lett.* **100**, 010402 (2008).
- [12] S. Basu and E. Mueller, arXiv:0712.1007.
- [13] M. J. Leskinen, V. Apaja, J. Kajala, and P. Törmä, arXiv:0802.1882.
- [14] C. A. Regal, M. Greiner, and D. S. Jin, *Phys. Rev. Lett.* **92**, 040403 (2004).
- [15] Q. J. Chen, I. Kosztin, B. Jankó, and K. Levin, *Phys. Rev. Lett.* **81**, 4708 (1998).
- [16] N. Andrenacci, P. Pieri, and G. C. Strinati, *Phys. Rev. B* **68**, 144507 (2003).
- [17] E. Taylor, A. Griffin, N. Fukushima, and Y. Ohashi, *Phys. Rev. A* **74**, 063626 (2006).
- [18] R. Haussmann, W. Rantner, S. Cerrito, and W. Zwerger, *Phys. Rev. A* **75**, 023610 (2007).
- [19] P. Nozières and S. Schmitt-Rink, *J. Low Temp. Phys.* **59**, 195 (1985).
- [20] Q. J. Chen, J. Stajic, S. N. Tan, and K. Levin, *Phys. Rep.* **412**, 1 (2005).
- [21] Here we extend this approximation above the actual T_c as well, to estimate Δ and μ .
- [22] R. Combescot, A. Recati, C. Lobo, and F. Chevy, *Phys. Rev. Lett.* **98**, 180402 (2007).
- [23] C. Chin and P. Julienne, *Phys. Rev. A* **71**, 012713 (2005).
- [24] J. O. Andersen, *Rev. Mod. Phys.* **76**, 599 (2004).